

# Energetics and structures of the tilted phases of fatty acid Langmuir monolayers

Óscar Toledano<sup>1</sup>, Miguel A. Rubio<sup>2</sup> and Óscar Gálvez<sup>1\*</sup>

<sup>1</sup> *Dpto. Física Interdisciplinar, Facultad de Ciencias, Universidad Nacional de Educación a Distancia (UNED), Senda del Rey, 9, 28040 Madrid, Spain*

<sup>2</sup> *Dpto. Física Fundamental, Facultad de Ciencias, Universidad Nacional de Educación a Distancia (UNED), Senda del Rey, 9, 28040 Madrid, Spain*

(e-mail: oscar.galvez@ccia.uned.es)

\*corresponding author

Key-words: Langmuir monolayer, fatty acids, dihydrogen interactions, tilted phases, DFT calculations.

## Abstract

Langmuir monolayers are monomolecular deep films composed of amphiphilic molecules which are typically confined to a water/air interface in a bi-dimensional structure. Due to the important applications in many research areas, they have been studied for many years. Their phase diagrams present several condensed phases, showing untilted or tilted structures at low values of surface pressure. In this paper, we present a novel density functional study on tilted phases of different fatty acid Langmuir monolayers. By means of this study, a further understanding of the physical chemistry properties and the nature of the formations of tilted monolayers can be achieved. Our calculations reveal that, regardless of the number of carbon atoms which form the apolar chain, the transversal (or conventional in the case of untilted phases) unit cell show similar dimensions, ca. 4.9 x 6.8 Å, which is in fair agreement with the range of the observed data. The energy variation of the unit cell as a function of the inclination of the molecules, reveal an abrupt increase in values larger than 45° and 36° for NN- and NNN-tilt, respectively, in fair agreement with the

experimental observation of  $L_{2h}$  (NN) and  $L_{2'}$  (NNN) phases of fatty acids. All of the fatty acids explored (from 10 to 19 carbon atoms) yield similar results. Finally, the energetics and structural changes of the monolayer along the variation of the area per molecule, obtained by enlarging in a-, b- or both axes of the untilted unit cell, have been explored. This study reveals that the untilted phases are energetically more stable at low values of the area per molecule (high surface concentration), as it is expected. When the area per molecule values are increasing, tilted phases (along NN or NNN-direction) with b/a ratio typical of herringbone (HB) or pseudo-herringbone (PHB) structures are found in the lowest energy configurations, which depend on how the distortion of the untilted unit cell is performed. For example, HB structures are the most stable when the molecules tilt along the enlarged axis of the untilted unit cell (a or b), meanwhile unit cell structures characteristic of PHB configurations occur in the opposite cases and at larger values of the area per molecule (low surface concentrations). All these predictions are in good agreement with the GIXD observations of the different phases of the phase diagram of fatty acid Langmuir monolayers.

## 1. Introduction

Langmuir monolayers are monomolecular deep films composed of amphiphilic molecules that are confined to a fluid/fluid interface. Such systems are crucial in many industrial processes in sectors such as cosmetics [1], food processing [2], and oil extraction and recovery [3]. Moreover, they are a key ingredient in life processes such as pulmonary function [4, 5], where the pulmonary surfactant allows for air filling the alveoli. In addition, they are very interesting systems from a more fundamental point of view because they are used as model systems of the cell membrane [6, 7] or as ideal systems to test theoretical predictions for the structural and dynamical properties of two-dimensional systems [8, 9].

Fatty acids are amphiphilic molecules that are formed by a polar “head” (the carboxylic group) and a nonpolar “tail” that is a saturated aliphatic chain. When placed in an interface

between a polar and a nonpolar media, the polar head prefers to stay inside the polar medium and, reciprocally, the nonpolar tail prefers to remain inside the nonpolar medium. Hence, the fatty acid chains are confined to the interface. In the most usual case of air/water interfaces, the polar (hydrophilic) head stays inside the water phase while the nonpolar (hydrophobic) tail lays inside the air phase.

The structure of the phase diagram of fatty acids Langmuir monolayers has been investigated mainly through thermodynamic measurements (compression isotherms [10]), that yield information on the critical values of the macroscopic variables and the order of the phase transitions, Brewster angle microscopy (BAM) [11], which reveals the tilted/untilted character of the different thermodynamic phases at the micron scale, and grazing incidence X-ray diffraction (GIXD) [8], which yields detailed information about the monolayer lattice structure at the molecular scale.

The general appearance of the phase diagram of a fatty acid Langmuir monolayer is shown in Fig. 1 (adapted from [8]), where the different phases are indicated and the tilted phases are labeled according to the tilt orientation as nearest neighbor (NN) or next nearest neighbor (NNN). Solid lines correspond to first order phase transitions and dashed lines to second order phase transitions. Highly condensed phases with all chains normal to the interface (untilted) appear at high interfacial pressures. Below a certain pressure threshold the molecules find more space and their chains show a tilt angle which depends on several factors, being the amphiphilic molecule concentration, the monolayer temperature and its functional group nature the most determinant ones [8]. The pressure threshold for the tilted phases to appear showing a slight temperature dependence [12].

GIXD studies provide a detailed knowledge of the monolayer structure of the different thermodynamic phases [13, 14, 15]. In the condensed phases the monolayer structure is an orthorhombic 2D lattice (determined by the cell parameters "a" and "b") with two molecules contained in each cell, one situated in one of the cell vertices and the other

roughly at the center of the cell. Moreover, the tilt orientation always points towards one of the two directions defined by the unit cell vectors **a** or **b** of the monolayer (see Fig. 1) [13, 14, 15].

The unit cell vectors **a** and **b** are the 2D lattice vectors on the surface, where the polar heads are placed, as shown in figure 2. In the tilted structures, we can also define the so-called transversal unit cell, in which **a<sub>⊥</sub>** and **b<sub>⊥</sub>** vectors are perpendicular to the carbon chain directions (Fig. 2). In these phases, two key angles,  $\phi_x$  and  $\phi_y$ , are defined, which determine the inclination and orientation of the carbon chains along the monolayer (see Fig. 3 and definitions of the tilt angles below). As mentioned above, depending on the direction of the tilt, two different kinds of structures are differentiated: when the tilt is aligned along the short size of the unit cell, **a**, they are denoted as NN (Nearest Neighbor) tilted phases, on the other hand, when the tilt occurs along the large size of the unit cell, **b**, a NNN (Next Nearest Neighbor) tilted phase is obtained.

Although the cell structures of the untilted phases are in general well-known [8, 16], both the atomic structure and the mechanism of formation of the tilted phases are much poorly understood. In physical terms, the actual tilt angle of the monolayer is typically fixed by the equilibrium distances of the inter-chain dihydrogen contacts (with H...H distances normally around 2.5 Å), which finally conducts to approximately constant values for the transversal unit cell vectors **a<sub>⊥</sub>** and **b<sub>⊥</sub>** [12, 17]. In Fig. 2 we can observe that the transversal unit cell vector oriented parallel to the tilt direction, **b<sub>⊥</sub>** in this case, is shrunk (**b<sub>⊥</sub><b**), while **a<sub>⊥</sub>**, preserves its initial value (**a<sub>⊥</sub>=a**).

Regarding the mutual orientation of the backbone carbon planes (defined as the plane, which contain all the carbon atoms along the molecule) in the unit cell, the so-called herringbone structures (with a mutual orientation of 90 degree) are typically obtained for phases at low temperature, i.e.: CS, S, L<sub>2</sub>'', L<sub>2</sub>', and L<sub>2h</sub> (see Fig. 1).

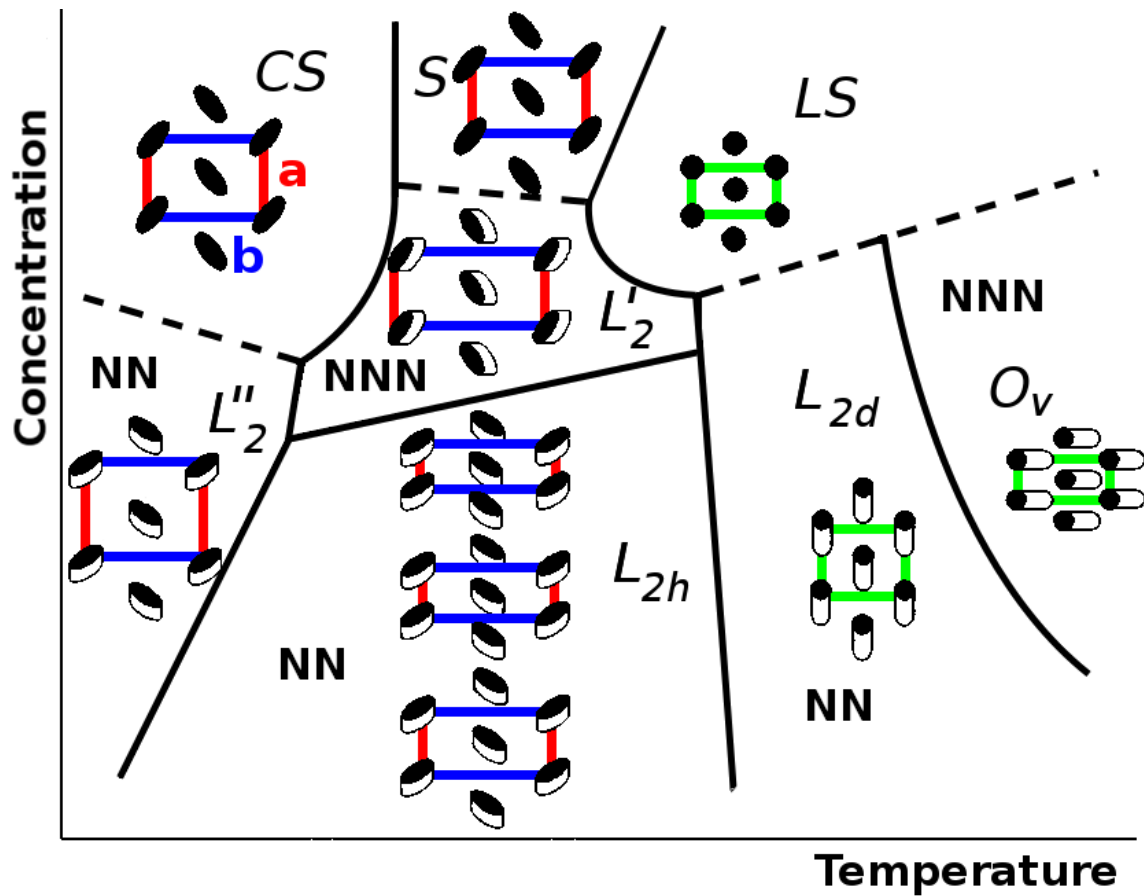


**Figure 1.** Generic phase diagram of fatty acids Langmuir monolayers, indicating the tilt direction for each phase. Nearest neighbor and next nearest neighbor tilted phases are indicated with NN and NNN respectively. The unit cell lattice parameters **a** and **b** are represented in red and blue, respectively. The unit cells of hexatic phases are in green. Figure adapted from ref [8].

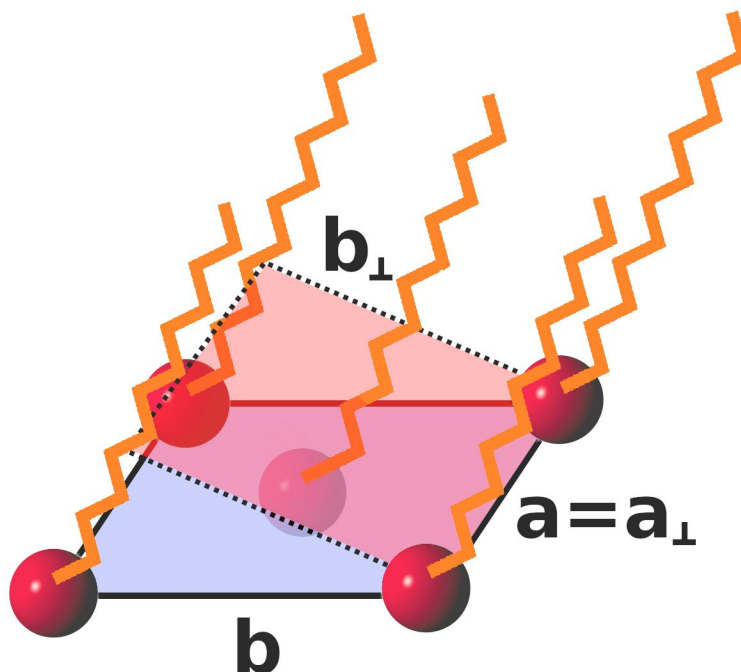


**Figure 2.** Representation of the unit cell (in blue) and transversal unit cell (in pink) with lattice parameters  $a$  and  $b$ ,  $a_{\perp}$  and  $b_{\perp}$  respectively. The carbon chain skeletons are represented in orange, and the polar heads, lying on the water surface, in red. In this case, the tilt is oriented along the  $b$  direction, so  $a_{\perp} = a$  and  $b_{\perp} < b$ .

The rich phase diagram of the Langmuir monolayers has been determined along the 30 past years, obtaining at least 4 different tilted phases [8], shown in figure 1. Phase  $L_2$  can be also divided into two different phases,  $L_{2h}$  and  $L_{2d}$ , which occur at low and high temperature respectively. The low temperature phase,  $L_2''$ , is tilted along the NN direction, and has a herringbone ordering. As the monolayer temperature is increased, a phase transition occurs either to the  $L_{2h}$  phase, at lower surface pressures, or to the  $L_2'$  phase, at intermediate values of the surface pressure. At the  $L_2''$ - $L_{2h}$  transition the tilt remains in the same direction, but the dimension of the cell changes abruptly, leading to a first order phase transition. At higher values of the surface pressure, the monolayer reaches the  $L_2'$  phase, whose tilt orientation points towards the NNN direction. For high temperature values, the  $L_{2d}$  phase appears, which shows hexatic order and is tilted towards the NN direction. At even higher temperatures and intermediate pressures, the  $O_v$  phase occurs, which is also hexatic but tilted in the NNN direction.

Generally speaking, one can summarize the aforementioned experimental information about the tilt angle by saying that tilt occurs in the NN direction at the lower surface pressure phases, while it flips to the NNN direction through a first order phase transition at intermediate values of the surface pressure. However, this is a too simple picture since the relation between the tilt angle and the surface pressure depends also on, both, the nature of the polar head and the chain length. For long chains, the transition from a tilted to an untilted phase appears to occur at a slightly higher surface pressure than for short chains [18]. This observation could be explained by the fact that the longer the chains the higher the pressure needed to overcome the larger number of inter-chain interactions occurring in the tilted phases.

In spite of the abundant experimental information about the tilted phases of fatty acid Langmuir monolayers, their physics is still poorly understood at the molecular level. In an interesting series of papers [19, 20, 21] Vysotsky et al. faced the problem of the structure and characterization of tilted phases using a semi empiric simulation method. Those works focused on the study of the energetics, structures, and thermodynamic barriers of the tilted aggregates of amphiphilic molecules with different polar heads for the first time. In spite of the limitations of the semi-empirical method employed, qualitatively good results were obtained for the different systems examined. However, in order to obtain a more realistic description of the structure and energetics of the Langmuir monolayers high level *ab initio* calculation need to be developed.

Recently, we have shown [16] that, both, a better description of the weak dihydrogen interactions that are present in these systems, and a more accurate representation of the structure of a large monolayer, using periodic conditions, can be obtained by using modern first principles simulation methods based on density functional theory. In that study, it was shown that dihydrogen contacts established among alkyl chains play a leading role in the final structure of the monolayer. In addition, different untilted structures for the high pressure phases, S and CS, were proposed.

In the present study, we report on a detailed analysis of the energetics and spatial structures of the tilted phases of different fatty acid Langmuir monolayers at different surfactant interfacial concentrations. This study aims at reproducing and understanding the phase diagram of the condensed phases at different surface pressures, i.e., at moderate and high interfacial concentrations, covering the whole range of concentrations shown in figure 1. Low surface concentration phases [11] (which are not included in figure 1), where the coexistence of domains of condensed and expanded liquid phases with different shapes and sizes may appear, are out of the scope of this investigation.

It is important to highlight that the molecular arrangement of the monolayer is determined both by the surfactant-surfactant interactions (lead by the dihydrogen contacts) and the interactions between the sub-phase and the surfactant (solvation). At low concentration, the solvation effects of the polar water sub-phase will cause the dispersion of the molecules of the monolayer all over the surface, decreasing the number of inter-chains interactions and giving place to a 2D-fluid phase when the surface pressure is low enough. On the contrary, in 2D-condensed phases inter-chain interactions become significant and amphiphilic molecules will cover the entire surface generating the tilted or untilted phases when the surface pressure is high enough. In our calculations, we have kept the concentration of molecules within an appropriate range, in which inter-chain interactions dominate to establish dihydrogen contacts. This situation is the opposite to that found for monolayers formed by nonpolar molecules, which show untilted structures, even at low surface pressure [22], where solvation effects are negligible and only surfactant-surfactant interactions are relevant.

Here we report on a study focused on the structure and stability of the tilted phases and their changes upon variation of the chain length and surface concentration. More specifically, by means of high level first principles simulations, we have studied the structure of the monolayers and their tilt angle orientations at different values of area per molecule,



which could be representative of different tilted phases. The paper is organized as follows. In section 3.1, we explore the dependence of the structure of the untilted cell upon the length of the carbon chain. In section 3.2, the energetics of the tilted structures at different concentrations, for a constant inter-chain distance, and with different chain length is analyzed. Section 3.3 includes the study of the monolayer structure and energetics at constant concentration, by varying the tilt angle to find the energetically most favorable structures. The discussion of all these results is incorporated into section 4. Finally the main conclusions of this work are gathered.

## **2. Computational Methods**

### **2.1. DFT calculations**

In order to understand the role of the different system parameters on the structure and stability of the tilted phases of fatty acid Langmuir monolayers, we have performed extensive first principle simulations in the framework of Density Functional Theory (DFT). Following the procedure of previous studies [16], we have used the vdW-DF-cx functional [23] to characterize the fatty acid monolayers. This functional, which belongs to the vdW-DF family, includes van der Waals contributions to the total energy, which are crucial to adequately simulate the dihydrogen interactions formed between hydrocarbon chains. These kinds of functionals require much larger computational time than GGA or hybrid functionals, but it has been demonstrated that the latter ones cannot fairly reproduce van der Waals interactions because they usually underestimate the dissociation energies [24, 25]. The performance of the vdW-DF-cx functional with the TZ basis set has been previously tested in alkane dimers systems, obtaining structural parameters and dimerization energies in fair agreement with those computed by CCSD(T)/MP2 methods with cc-pVDZ or cc-pVTZ basis sets [16].

In this work, the SIESTA (Spanish Initiative for Electronic Simulations with Thousands of Atoms) package has been used to perform the DFT calculations, which includes the vdW-DF-cx functional mentioned above and Gaussian-type Numerical Atomic Orbital (NAO) as

basis sets. The Troullier-Martins norm-conserving pseudopotentials [26], which are implemented in SIESTA, are selected to simulate the core electrons interactions. As the dihydrogen contacts lead to intermolecular H...H distances ranging from 2.5-3.0 Å (with low values of interaction energies per contact of around 1 meV), the basis set selected must be very flexible and large to accurately reproduce the electronic density for this kind of interactions [27]. Thus, we have employed the TZP (triple zeta with polarization) basis set implemented in the SIESTA package, which provides a satisfactory flexibility for this kind of systems [16]. The cutoff radius of the numerical orbitals is fixed to an energy shift of 1 meV (this quantity measures the difference between the full and the truncated orbital energies), which yields to a rather extended basis set. The real space grid is fixed to 300 Ry and the reciprocal space sampling is performed with a grid cutoff of 8 Å. The structure optimizations are achieved with force tolerance parameters of 0.01 eV/Å and 0.001 eV/rad.

It is important to clarify that our methodology does not take into account any temperature or solvation effect in the monolayer simulation, which cannot be fairly simulated with high-level DFT calculations in this approximation.

## 2.2. Analysis procedures

In order to determine the tilt magnitude and direction, as well as the conventional and transversal unit cell vectors, the tilt angles  $\phi_x$  and  $\phi_y$  along the  $x$  and  $y$  directions (parallel to **a** and **b** vectors respectively) are specified.  $\phi_x$  is defined as the angle between the  $z$ -axis and the projection of the chain direction in the  $XZ$  plane, as is shown in figure 3. In an analogous way,  $\phi_y$  is defined as the angle between the  $z$ -axis and the projection of the chain direction in the  $YZ$  plane (see Fig. 3). Note that typically  $\phi_x$  and  $\phi_y$  refer to the inclination along the NN and NNN directions respectively. Using these two values, the tilt of the carbon chain, defined as the polar angle  $t$ , and the orientation of the tilt, given by the azimuthal angle  $\theta$ , can be determined by:

$$\theta = \arctan\left(\frac{\cot(\phi_x)}{\cot(\phi_y)}\right)$$

(1)

$$t = 90 - \arctan(\sin(\theta) \cdot \cot(\phi_y))$$

The lengths of the transversal and conventional unit cell vectors are also related by:

$$|a_{\perp}| = |a| \cdot \sin(\theta) \cos(\phi_y)$$

(2)

$$|b_{\perp}| = |b| \cdot \cos(\theta) \cos(\phi_x)$$

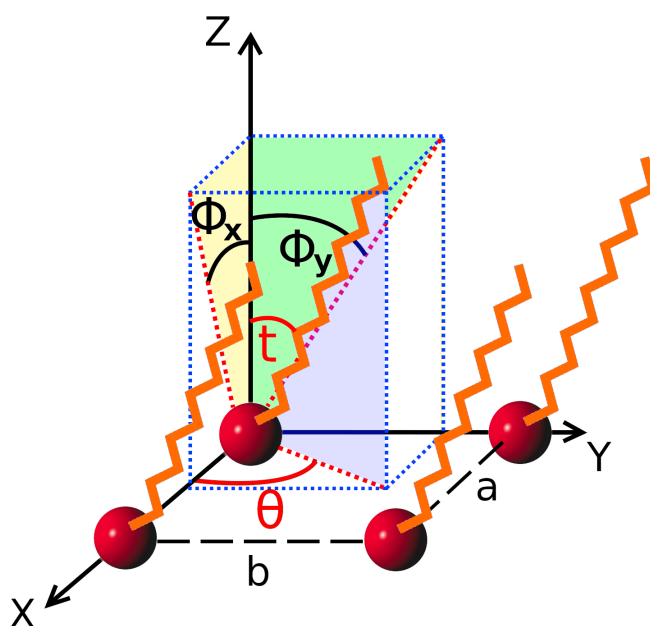


**Figure 3.** Representation of the tilt angle,  $t$ , of the chain direction relative to the interface. The azimuth of the tilt direction is named as  $\theta$ , which is the angle between the x-axis and the projection of the chain direction in the XY plane. The projected angles  $\phi_x$  and  $\phi_y$  are represented in black, and are defined between the x- and y-axis and the projection of the chain direction into the XZ and YZ planes respectively. In this figure the central molecule of the unit cell is not shown for clarity (see Fig.2).

Having this in mind, we have devised three different analysis schemes:

- a) Structure and energetics of the untilted phases: Before analyzing the tilted phases, we study the structure of the unit cell for the untilted phases of fatty acid monolayers, for different chain lengths ranging from 10 to 20 carbon atoms. To

optimize the unit cell structure, several relevant parameters identified in our previous work [16] will be varied in the optimization process. These parameters are: the cell lengths  $|\mathbf{a}|$  and  $|\mathbf{b}|$ , the relative position of both molecules  $\mathbf{r}$ , the azimuthal orientations of the backbone carbon planes of each of the two molecules of the unit cell  $\alpha_{1,2}$ , and the dihedral angles of the carboxylic groups  $d_{\text{COOH}}$  (see Fig. 5 and 10 in ref. [16]).

- b) Analysis of the energetics and structure of the tilted monolayers at constant transversal unit cell ( $\mathbf{a}_\perp$  and  $\mathbf{b}_\perp$ ): In this case,  $\mathbf{a}$  and  $\mathbf{b}$  are varied, and consequently the surface concentration is also changed. In principle, there are two ways in which this analysis could be carried out: i) to displace the molecules along the  $\mathbf{a}$  and/or  $\mathbf{b}$  directions varying the tilt angles  $\phi_x$  and/or  $\phi_y$  appropriately so as to keep  $\mathbf{a}_\perp$  and  $\mathbf{b}_\perp$  constant, and ii) displacing the molecules along the z-axis, in a similar way to that proposed by Vysotsky *et al.* [19]. In both cases the inter-chains distances, and thus  $\mathbf{a}_\perp$  and  $\mathbf{b}_\perp$ , remain constant, whilst the surface concentration, determined by the product of  $\mathbf{a}$  and  $\mathbf{b}$  lengths, is varied. In this study, the tilt is produced in only one direction, so the transversal and the conventional unit cell will follow the relation:

$$\frac{a_\perp}{a} = \cos(t) \quad (3)$$

For simplicity, in this work, we have followed the procedure proposed by Vysotsky *et al.* It is important to highlight, that during this procedure the geometry and orientation of both molecules of the unit cell are fixed to those of the untilted structure.

- c) Analysis of the energetics and structure of the tilted monolayers at constant surface concentration (determined by the product of  $|\mathbf{a}\times\mathbf{b}|$ ): In this case, the inclination angles,  $\phi_x$  and/or  $\phi_y$  are optimized in the minimization process. In an orthorhombic cell, there are infinite combinations of  $|\mathbf{a}|$  and  $|\mathbf{b}|$  values that yield the same concentration. Hence, we will only analyze three representative cases: two in which

the unit cell is distorted only along one axis (taking as reference the untilted unit cell parameters), and another in which both axis are distorted simultaneously in the same way. As in the previous case, during these calculations the geometry and orientation of both molecules of the unit cell are fixed to those of the untilted structure.

### 3. Results

#### 3.1. Untilted Structures: Chain Length Dependence

The results obtained for the untilted monolayers of the different fatty acids according to procedure a) are summarized in table 1. Here we have defined  $\Delta E_{\text{cell}}$  as the difference between the energy of the unit cell (which includes two molecules) in the minimum energy configuration and that of the two isolated molecules. From the results showed in table 1, we can see that the structural parameters of the unit cell for all fatty acids are very similar. Moreover,  $\Delta E_{\text{cell}}$  grows linearly with the chain length for the fatty acids explored in this study, keeping constant the  $\Delta E_{\text{cell}}$  value per carbon unit in the chain, i.e.  $\Delta E_{\text{C-cell}}$ , (approx. -0.26 eV), defined as the ratio between  $\Delta E_{\text{cell}}$  and the number of carbon atoms (see Table 1).

**Table 1.** Structural parameters and energetics of the untilted fatty acids monolayers for chain length ranging from 10 to 20 carbon atoms.  $\Delta E_{\text{cell}}$  is the energy difference between the unit cell and two isolated fatty acid monomers, and  $\Delta E_{\text{C-cell}} = \Delta E_{\text{cell}}/n$ , where  $n$  is the number of carbon atoms in the fatty acid chain. Distances are in Å, areas in Å<sup>2</sup>, angles in degrees, and energies in eV.

Fatty Acid	a	b	b/a	Area per molecule	$\alpha_1$	$\alpha_2$	$d_{\text{COOH-1}}$	$d_{\text{COOH-2}}$	$\Delta E_{\text{cell}}$	$\Delta E_{\text{C-cell}}$
10	4.90	6.80	1,39	16,6	44,4	135,7	17,9	-18,5	-2,58	-0,258
12	4.90	6.73	1,37	16,5	44,7	135,4	22,8	-22,9	-3,10	-0,258
14	4.95	6.77	1,37	16,8	44,6	135,6	23,2	-22,9	-3,62	-0,259
16	4.88	6.77	1,38	16,5	44,4	135,5	22,3	-22,3	-4,17	-0,260

18	4.96	6.78	1,37	16,8	44,6	135,2	22,8	-23,2	-4,69	-0,261
20	4.90	6.84	1,40	16,8	44,6	136,8	15,2	-20,6	-5,19	-0,260
Mean	4.92	6.78	1,38	16,7	44,6	135,7	20,7	-21,7		-0,259

The mean values of the unit cell dimensions collected in Table 1 are ca. 4.9 x 6.8 Å, which are in fair agreement with the observed values (approx. 5.0 x 7.5 Å measured at 10 °C [8, 17]), being the largest differences for the longer axis b. Our methodology does not take into account any temperature or solvation effect in the monolayer simulation, and it would be expected to obtain larger lattice parameters at temperatures ranging from 0 °C to 40 °C or when a solvation medium is included. In fact, this elongation is expected to be larger for longer intermolecular distances (and weaker dihydrogen interactions). Consequently, as larger intermolecular distances are obtained in axis b, the temperature or solvation effect should be more noticeable in this axis, according to our results.

The energy  $\Delta E_{\text{cell}}$  grows monotonously with the size of the carbon chains (see Table 1). As mentioned before, the formation of the monolayer is due to the balance of inter-chain, polar heads and surfactant-subphase interactions. In the case of different fatty acids, the solvation effects and polar heads interactions should be similar, but the inter-chain interactions are larger for longer carbon chains (due to more dihydrogen contacts are formed), as is shown in table 1. During the transition from tilted to untilted phase (or vice versa) it is necessary to break and form new interactions. As longer chains have a higher number of dihydrogen contacts (and stronger inter-chain interactions), it is conceivable that for longer chains one would need higher surface pressures to overcome these higher energetic barriers, in agreement with the experimental findings [18]. We will explore this effect also in the case of the formation of tilted phases in the following sections.

### 3.2. Tilted Structures: constant transversal unit cell

In this section, the energetics of the tilted structures at constant transversal unit cell ( $\mathbf{a}_\perp$  and  $\mathbf{b}_\perp$ ) are studied and the concentrations, determined by the product of  $|\mathbf{a}_\perp \times \mathbf{b}_\perp|$ , will be varied.

The experimental observations of the Langmuir monolayers show that the transversal unit cell area is approximately constant for the different fatty acids studied, ranging from 38-42  $\text{\AA}^2$  [17]. This observation is in good agreement with our calculations (see next section). The observed arrangements of the molecules (the backbone plane orientations) inside the unit cells show typically three different configurations, which lead to different  $b_\perp/a_\perp$  ratios. For high temperatures, hexatic phases are observed, following the relation  $b_\perp = \sqrt{3}a_\perp$ , in which the backbone carbon planes could rotate around their axis. At low temperatures, the observed unit cell presents a herringbone arrangement (HB), with the backbone planes forming a  $90^\circ$  angle and with a distinctive ratio  $b_\perp \simeq 1.5a_\perp$ , or a pseudo herringbone arrangement (PHB) with backbone planes forming angles of ca.  $55\text{-}65^\circ$  and with the lattice parameter ratio  $b_\perp \simeq 2a_\perp$  [28].

For this study, we have defined  $\Delta E_{\text{tilt}}$  as the energy difference between tilted and the untilted structures (both with the same transversal unit cell), namely,  $\Delta E_{\text{tilt}} = E_{\text{tilted}} - E_{\text{untilted}}$ .  $\Delta E_{\text{tilt}}$  is expected to be larger as the tilt increases because the number of dihydrogen contacts between chains is reduced. In Figures 4a and 4b, we show the dependence of  $\Delta E_{\text{tilt}}$  on the tilt angles  $\phi_x$  and  $\phi_y$  (or the area per molecule) for the different fatty acids here studied. A first observation indicates that  $\Delta E_{\text{tilt}}$  is always positive. Hence, the untilted structure appears to be always the most stable one. This finding is contradictory with the experimental observations, but it could be explained by the absence of the solvation and temperature effects in our simulations.

According to the results in Figure 4, (see panel 4c) from an expanded liquid phase and increasing the surface pressure (so the area per molecule is reduced) at tilt angles around  $45^\circ$  (area per molecule of ca.  $24 \text{\AA}^2/\text{molecule}$ ), a local minimum of  $\Delta E_{\text{tilt}}$  is obtained for inclinations along x-axis (NN), showing  $\Delta E$  values considerable lower than monolayers tilted along y-axis (from 0.1 to 0.5 eV depending on the direction and orientation of the tilt). This

result suggests that NN phases should be first formed in the fatty acid monolayers when the surface pressure is increased (see panel 4c), and in fact, the observed findings show that  $L_{2h}$  (NN) phase appears at a lower surface pressure than  $L_{2'}$  (NNN) [8, 29], in agreement with our calculations.



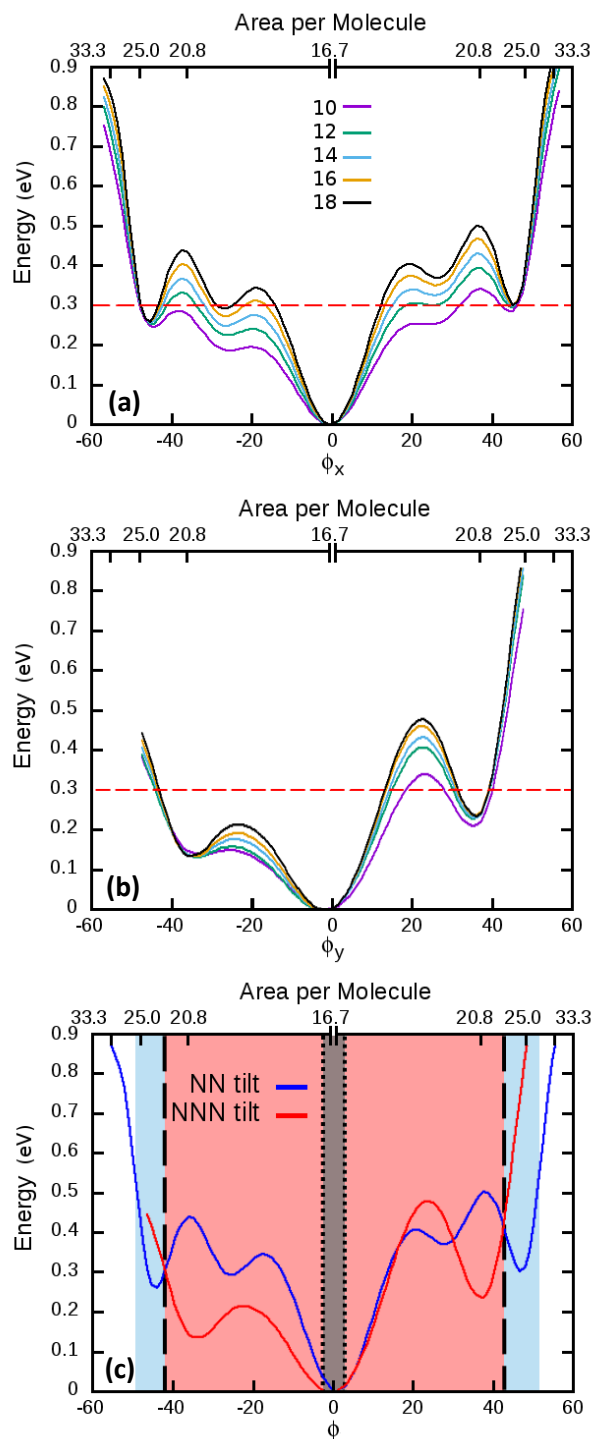


**Figure 4.** Energy differences,  $\Delta E_{\text{tilt}}$  (in eV), between the tilted and untilted structures along the inclination angles  $\phi_x$  (a) and  $\phi_y$  (b), defined in Fig. 3, for different fatty acid monolayers with hydrocarbon chain ranging from 10 to 18 carbon atoms. The area per molecule in  $\text{\AA}^2$  is also indicated in the upper scale. A red dashed line is drawn at 0.3 eV just to guide the eye. Panel c shows a comparison for the case of C18. Colored areas indicate the region in which NN, NNN or untilted structures are energetically more stable (in blue, red and grey respectively)

Moreover, Figure 4 shows that  $\Delta E_{\text{tilt}}$  increases abruptly for inclinations larger than ca.  $45^\circ$  and  $36^\circ$  for  $\phi_x$  (NN) and  $\phi_y$  (NNN), respectively. This result could indicate that only structures with tilt angles lower than these values should be expected to occur in the monolayer. In fact, the observed maximum values for  $L_{2h}$  (NN) and  $L_{2'}$  (NNN) for different fatty acids [12] are ca.  $35^\circ$  and  $20^\circ$  respectively, which are included in the low  $\Delta E$  range (lower than 0.3 eV) obtained in our calculations. The discrepancy between experimental and calculated values of the maximum tilt angle could be explained by simple geometrical considerations. In the inclination process of the molecules in the unit cell some dihydrogen contacts are lost, which causes a decrease of the interaction energy among molecules. However, at a given tilt angle, the number of dihydrogen interactions lost also depends on the initial separation of the molecules (i.e. **a** and **b** values in the unit cell). Due to our calculated **a** and **b** values are shorter than experimental ones, it is reasonable that our simulations predict larger tilted angles than those measured experimentally to produce a notable destabilization of the structure.

It is important to clarify that, because of the computational cost, in the calculation of the curves in Figures 4 only the corresponding tilt angle has been allowed to vary, as it was described in section 2.2. This means that, once the tilt was imposed, no relaxation of the structure as e.g. regarding the orientation of the backbones planes was allowed. If such relaxation would be done the energy barriers appearing in Figures 4 might be somewhat reduced [16].

The remarkable asymmetry in the curves shown in Fig. 4b for tilts along the y-axis, compared to that in the x-direction (Fig. 4a) can be understood in terms of the anisotropy of the molecular arrangement in the unit cell, in which the polar heads point both in the same orientation along the y-axis, so inclinations along the positive direction of y-axis yield geometric arrangements significantly different from the corresponding to inclinations along the negative part of the y-axis. In the x-axis this effect is not observed because each molecule in the unit cell is pointing in opposite directions along this axis, so inclinations along both directions of this axis are qualitatively similar.

### 3.3. Tilted Structures: constant concentration

In the previous section, we evaluated the energetic of different tilted structures which preserved the area of their transversal unit cell. In this section, we will study the energetics and structures of the monolayer at fixed values of concentration (area per molecule), determined by the modulus of the vector product of the lattice vectors, namely  $|\mathbf{a}\times\mathbf{b}|$ . By means of this study, the structures and tilt angles of the monolayer at a given area per molecule can be obtained. However, for each concentration, infinite combinations of  $\mathbf{a}$  and  $\mathbf{b}$  values in an orthorhombic cell exist, hence, we have restricted our exploration to three representative cases, all of them starting from the values obtained for the untilted unit cell (i.e. 4.9 and 6.8 Å): i) elongation only along x-axis, ii) elongation only along y-axis, and iii) elongation along both axis proportional to their original values in the untilted configuration. For each one of these distorted unit cells,  $\phi_x$  and  $\phi_y$  angles have been varied to find the minima structures, which is equivalent to tilt the molecules along the NN and NNN directions, respectively. We remind the reader that due to the high computational cost of this study, the molecules of the unit cell are fixed to the geometry and orientation of the untilted structures, so backbone carbon planes of both molecules are constrained to be mutually oriented at 90°.

In high concentrations, i.e., low values of area per molecule, it is expected that untilted structures are the most stable, while for low concentrations, different minimum configurations, with the tilt pointing towards the NN or NNN or both directions, and with  $b_{\perp}/a_{\perp}$  ratios corresponding to a HB or PHB arrangement [8], might appear. Hexatic phases, which would require the inclusion of temperature and solvation effects in the simulation, cannot be studied by means of our computational method. A Molecular Dynamic or a Monte Carlo simulation might be more appropriate for this task.

These calculations have been carried out for areas per molecule ranging from 16.7 Å<sup>2</sup>/molecule (which correspond to the untilted HB structure, see Table 1) to 30 Å<sup>2</sup>/molecule. Because of the computational cost of the calculations, this thorough study, spanning a wide

range of values of the area per molecule, has been only done for the decanoic acid ( $C_9H_{19}COOH$ ), and the results are shown in Fig. 5 and 6. However, simulations in some particular unit cell areas have been also carried out in the case of eicosanoic acid ( $C_{19}H_{39}COOH$ ), obtaining analogous results and conclusions than for decanoic acid. Hence, we believe that the results may be safely presumed to have general validity for the range of fatty acid previously studied

Figure 5 shows the  $\Delta E_{\text{tilt}}$  contour maps of three different unit cells (distorted in **a**, **b** or both axes, see above), at three different concentrations, upon variation of  $\phi_x$  and  $\phi_y$  angles. As in Fig. 4,  $\Delta E_{\text{tilt}}$  refers to the energy difference between the tilted and the untilted configuration for each unit cell simulated. In all panels in Figure 5 the color coding assigns red and blue colors to the lowest and highest energy differences, respectively. The unit cell structures of the lowest energy configurations, corresponding to the four different kinds of tilted structures, from several views, are shown in Figure 6.

For the highest concentrations represented,  $17.5 \text{ \AA}^2/\text{molecule}$ , the values of  $\Delta E_{\text{tilt}}$  are positive for  $\phi_x$  and  $\phi_y \neq 0$  (see panel a in figure 5), which means that the untilted structures are more likely to be found than the tilted ones. The corresponding untilted structure can be observed in panels 1A and 1C of Figure 6.

For the lowest concentration represented,  $25 \text{ \AA}^2/\text{molecule}$ , (see panel c in Fig. 5), the inclination of the molecular chains (both the value of the tilt angle and the orientation) which yield the energy minimum structures depends on how the unit cell is distorted: along the x-axis (NN), y-axis (NNN) or both axis (column 1, 2 or 3 in Fig 5 respectively). The corresponding structures of the minima are shown in rows 2 and 3 of Fig. 6. One would expect that the tilt orientation of the chains would occur along the elongated axis of the unit cell, in order to preserve the inter-chain distances and the area per molecule of the transversal unit cell [8]. In fact, this is the case when the y-axis is elongated (corresponding to a NNN-tilt), obtaining the most stable structures for azimuth angles pointing to the distorted y-axis (see panel 2c in Fig. 5 which correspond to the structure shown in row 3 in Fig. 6).

Interestingly, in the case of elongations of the unit cell along the x-axis, energy minimum configurations with inclination along the x-axis are also predicted (as is shown in row 2 in Fig. 6), as expected, but, in addition, other energy minimum structures with inclinations along both axes (or even close to only y-axis) are also found (see the color map shown in panel 1c of Fig. 5). These new local minimum configurations yield transversal unit cell values of approx.  $4.6 \times 8.1 \text{ \AA}$  ( $b_{\perp}/a_{\perp} = 1.8$ ), which are similar to tilted phases with PHB transversal unit cells. In fact, the observed values of PHB structures are ranging in ca.  $4.5\text{-}4.6 \times 8.7\text{-}8.8 \text{ \AA}$  [28]. The major difference between experimental data and the results reported here concerns again the longer axis of the lattice and it could be due again to temperature or solvation effects (see discussion for untilted structures in section 3.1).

When the elongation of the unit cell is applied in both axis (panel 3c in Fig. 5), the most stable structures show tilts pointing to the intermediate directions between x- and y-axes, as we show in row 4 in Fig. 6. However, in this case, because the inclination and distortion occur both in the same direction, the transversal unit cell shows values typically corresponding to HB structures ( $b_{\perp}/a_{\perp} \approx 1.4\text{-}1.5$ ).

For the intermediate concentrations, row b in Fig. 5, the energy minimum structures always show inclinations values along the distorted axis, when only one is elongated, or along both axis when the distortion is applied for both directions, so typical  $b_{\perp}/a_{\perp}$  ratios of HB structures are found ( $b_{\perp}/a_{\perp} \approx 1.4\text{-}1.5$ ).

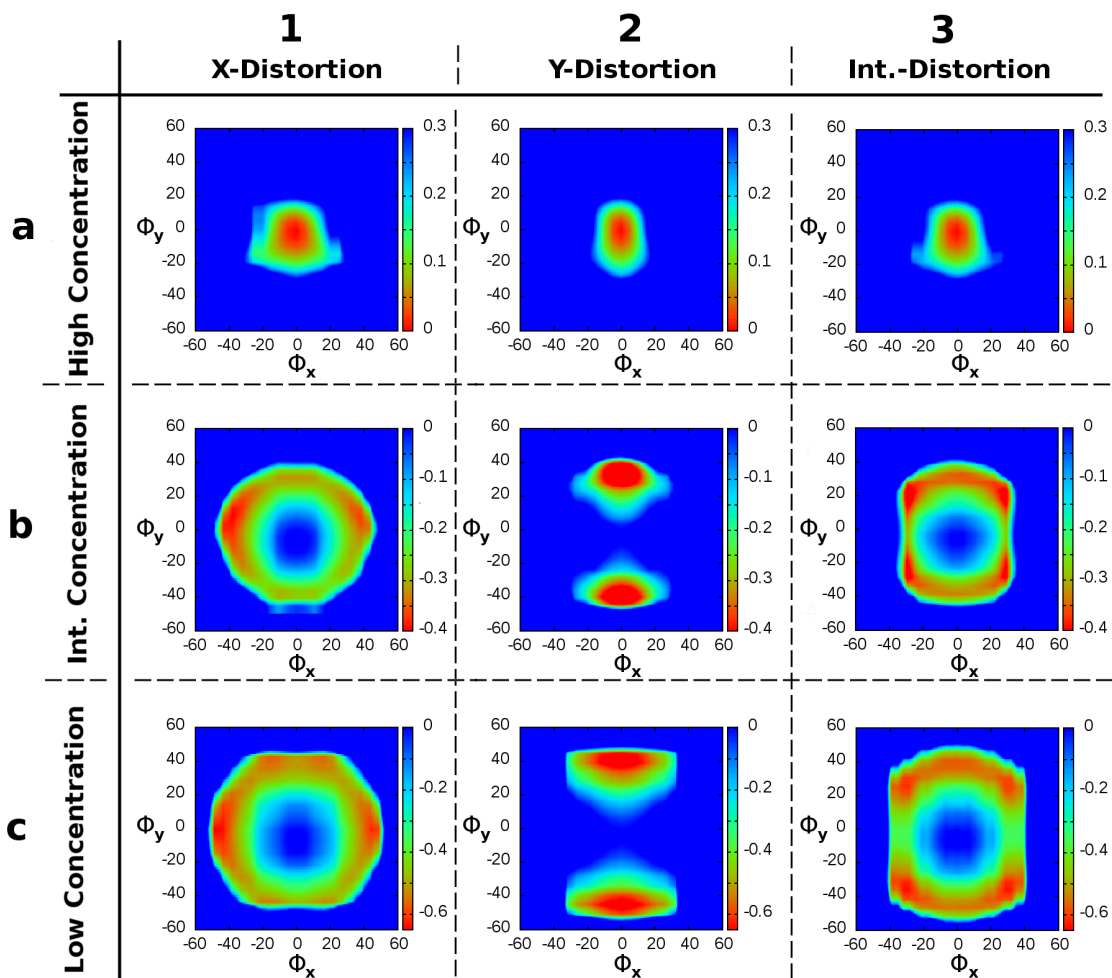


**Figure 5.** Energy difference,  $\Delta E_{\text{tilt}}$ , (in eV in the color scale) between configurations of a decanoic acid monolayer at different inclination angles  $\phi_x$  (horizontal coordinates) and  $\phi_y$  (vertical coordinate), and the untilted structure, for area per molecule of  $17.5 \text{ \AA}^2$  (high concentration, row a),  $22.5 \text{ \AA}^2$  (intermediate concentration, row b), and  $25 \text{ \AA}^2$  (low concentration, row c). Columns 1, 2 and 3 refer to the elongation of the unit cell imposed along x-axis, y-axis, or both axes, respectively.

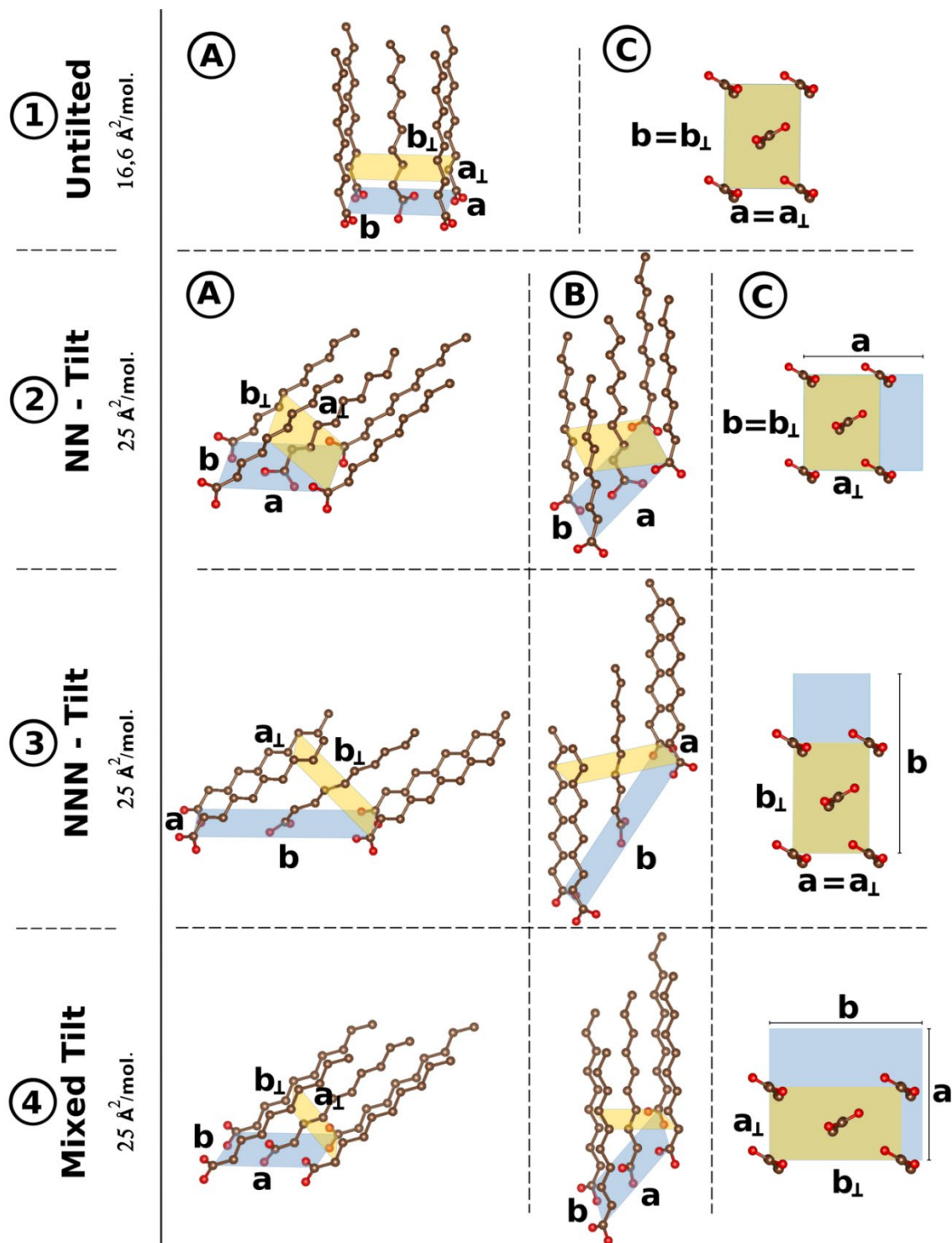


**Figure 6.** Representation of the unit cell for minimum configurations of a decanoic acid monolayer at four representative configurations (rows 1 to 4; with areas per molecule ranging from 16.6 to 25 Å<sup>2</sup>) with transversal cell plane in orange and conventional plane cell in blue. Side views parallel to the conventional or transversal unit cell plane in panel a and b respectively. Panel c shows a view from the top and perpendicular to the transversal cell plane. Red and grey beads represent oxygen and carbon atoms respectively.

In Figure 7 we plot the dependence of the relevant parameters ( $b_{\perp}/a_{\perp}$  ratio, energy differences, tilt and azimuth values in panels a, b, c and d, respectively) for the lowest energy configuration obtained (always a HB-type structure) in each of the three different unit cells simulated (distorted in the x-axis, y-axis, and both axes), on the area per molecule (inverse of the concentration). In this case, energy difference is named  $\Delta E_{\text{tilt-ab}}$  and it refers to the energy differences between the most stable configuration for each value of the area per molecule and the untilted structure of the optimized unit cell: 4,9 x 6.8 Å, which is in fact the global minimum of the monolayer structure. For some of the distorted cells (panels 1b, 3b, 1c and 3c in Fig. 5) several energy minimum structures, with very similar energy values, are found due to the symmetry of the system; in such cases only one of these equivalent minima has been considered in this analysis.



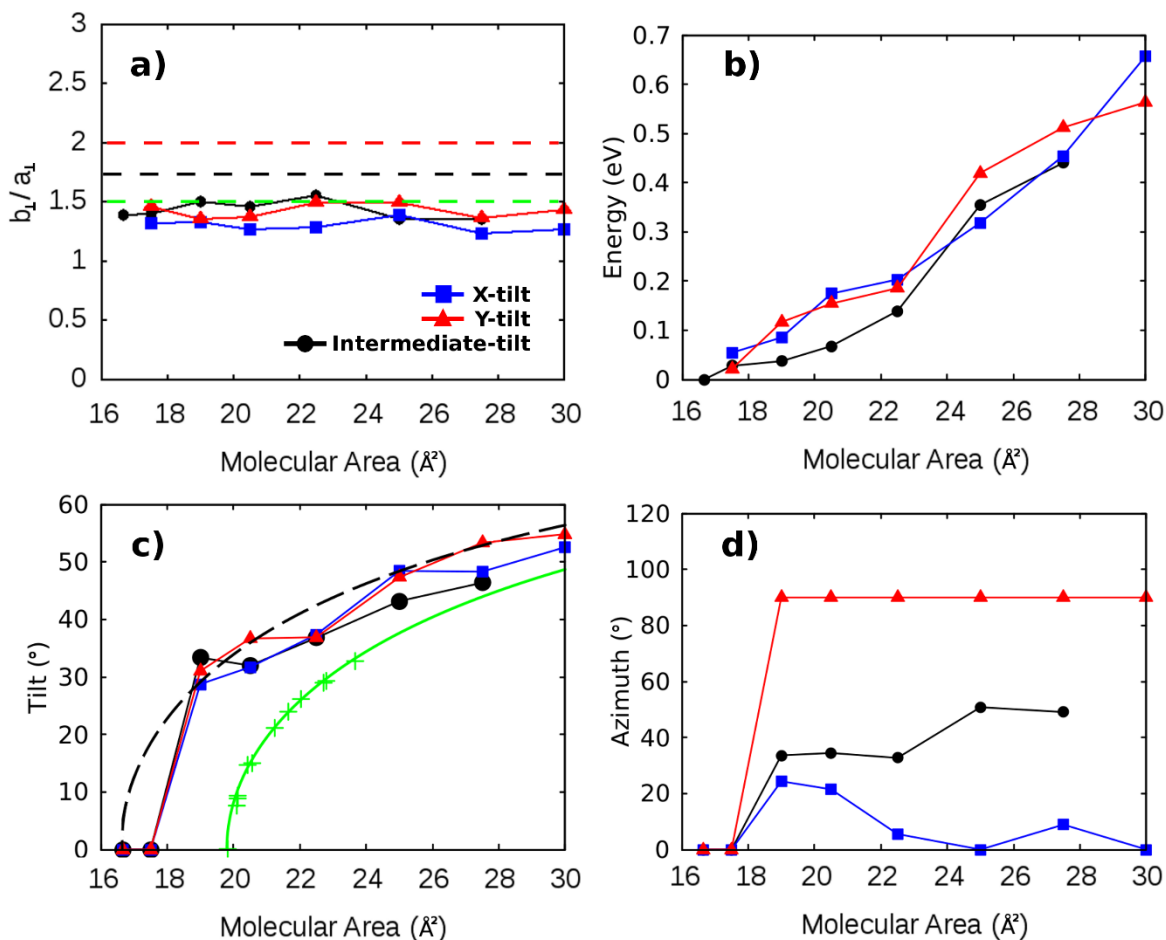


**Figure 7.** The influence of the area per molecule (in  $\text{\AA}^2/\text{molecule}$ ) on (a)  $b_{\perp}/a_{\perp}$  ratio, (b)  $\Delta E_{\text{tilt-ab}}$  (in eV), (c) tilt angle, and (d) azimuthal angle, (both in degrees), for the lowest energy configurations of three distorted unit cell (in the x-axis, y-axis, and both axes in blue, red and black curves respectively). See definition of  $\Delta E_{\text{tilt-ab}}$  in the text. Dashed colored lines in panel a refer to  $b_{\perp}/a_{\perp}$  ratio values of 2,  $\sqrt{3}$  and 1.5. Dashed black line in panel c represents computed data according to eq. 3 and green curve is experimental data from ref. [13].

Figure 7a shows that all the minimum structures presents similar  $b_{\perp}/a_{\perp}$  ratios for all the area per molecules values explored, in good concordance with the experimental findings [17]. These values are in a range of ca. 1.3-1.5 and they are typical of a HB configuration, as mentioned before.

It can be observed (see Figure 7b) that the energy of the minimum configurations grows (the structures are energetically less favorable with respect to the global minimum, i.e., the untilted structure) upon increasing the area per molecule for the three elongated unit cells studied, which correspond to elongations along the x-axis (blue trace), y-axis (red trace), and both axes (black trace), respectively. Interestingly, at the same area per molecule, the  $\Delta E_{\text{tilt-ab}}$  values corresponding to the three possible distorted unit cell are very similar (the differences are lower than 0.12 eV, around 4-5  $k_B T$ ). Here again, we remind that in these calculations the mutual orientation of the backbone carbon plane is fixed (at  $90^\circ$ ) because of the computational cost. It might well be that allowing for the relaxation of the carbon backbone plane might reveal energy differences among the three distorted structures. In any case, the energy differences found are smaller than  $5k_B T$  at temperatures around 300 K. Hence, any of these configurations could take place at room temperature.

The dependence of the tilt angle of the minima configuration of the area per molecule of each distorted unit cell is shown in Figure 7c. At high concentration (low values of area per molecule), the tilt angle is strictly null for values of the area per molecule lower than  $17 \text{ \AA}^2/\text{molecule}$ . Above that value, the tilt angle changes abruptly from  $0^\circ$  to  $30^\circ$  upon a small increase of the area per molecule (from  $17.5$  to  $19 \text{ \AA}^2/\text{molecule}$ ). Dashed black trace is the representation of the tilt angles obtained by eq. (3) keeping constant the transversal unit cell area to the value obtained at the untilted configuration,  $16.6 \text{ \AA}^2/\text{molecule}$ . Experimental studies [13] show that the surface pressure undergoes a large increase when the areas per molecule are in the range of  $20\text{-}23 \text{ \AA}^2/\text{molecule}$ , which correspond to the transition between untilted and tilted phases yielding an increase of the tilt angle from  $0^\circ$  to ca.  $33^\circ$ . Such experimental data are represented in green trace in Figure 7c for comparison, and they are in good qualitative agreement with our calculations. Here, the smaller **a** and **b** lengths consistently obtained in our simulations with respect to the experimental ones

result in smaller areas per molecule ( $17.5\text{-}19 \text{ \AA}^2$ ) when compared with those experimentally observed ( $20\text{-}23 \text{ \AA}^2$ ). Moreover, if we shift the experimental data around  $3 \text{ \AA}^2$  to the left, the qualitative agreement with our prediction is notable.

In Figure 7d we plot the orientation of the tilt corresponding to the energy minimum structures as a function of the area per molecule for the distorted unit cells in the x-axis, y-axis, and both axes (in blue, red, and black curves respectively). The tilt orientation in the conventional plane is given by the azimuth angle, which takes values from  $0^\circ$  to  $90^\circ$ , corresponding  $0^\circ$  and  $90^\circ$  to orientations along the x-axis and y-axis, respectively.

Figure 7d shows unambiguously that, as we mentioned before, elongations of the unit cell along y-axis (red curve in Figure 7d) yield always minima configurations with azimuth angles of  $90^\circ$ , that corresponds to an NNN structure. When the distortion of the unit cell is along the x-axis (blue curve in Fig. 7d), minima configurations show azimuthal angles lower than  $25^\circ$  and approaching to  $0^\circ$  (NN tilted structure) at large values of the area per molecule (low surface concentrations). For structures with a unit cell distorted in both axes (black curve in Figure 7d) azimuth values range from  $35$  to  $55^\circ$ , confirming that the orientations of the tilt is neither NN nor NNN.

#### 4. Discussion

Fatty acid monolayer have been analyzed attending to three different aspects.

First, we have studied the effect of the chain length in the untilted phases of the monolayers. The calculated values of the unit cell dimensions for all the fatty acids studied (with chain lengths ranging from 10 to 20 carbon atoms) are quite similar, being the mean value ca.  $4.9 \times 6.8 \text{ \AA}$ , which is in fair agreement with the range of the experimental values (approx.  $5.0 \times 7.5 \text{ \AA}$ , at  $10 \text{ }^\circ\text{C}$  [8]). The discrepancies could be justified by the absence of thermal or solvation terms in our simulations. In addition, our calculations show a monotonic increase of the energy values of the unit cell when the carbon chain length is

augmented, yielding an approximately constant value of -0.26 eV per carbon unit added. This linear growth of the energy with the number of carbon atoms forming the nonpolar tail is a direct consequence of the linear increase of the dihydrogen contacts which are responsible for the interaction between the molecules.

Second, concerning tilted phases, we have explored the dependence of the energy of the unit cell on the inclination of the molecules (in the x and y axes), keeping constant the transversal unit cell. This analysis has revealed that  $\Delta E$  variations are qualitatively similar for all the fatty acids studied (independent of chain length), showing an abrupt increase for inclinations larger than  $45^\circ$  and  $36^\circ$  for  $\phi_x$  (NN) and  $\phi_y$  (NNN), respectively. This result is in qualitative agreement with the experimental observations, which show maximum tilt values ca.  $35^\circ$  and  $20^\circ$  for the  $L_{2h}$  (NN) and the  $L_2'$  (NNN) phases, respectively [12]. The difference obtained could be due to our calculated **a** and **b** cell vectors are shorter than the experimental ones due to temperature or solvent effects which are not included in our methodology. In addition, our calculations also predict that NN phases (instead of NNN) should be the first liquid condensed phase to appear from an expanded liquid phase when the surface pressure is increased, in agreement with the experimental findings [8, 29].

Third, we have studied the energetics and structures of the monolayer upon variation of the area per molecule. Such variation was imposed by enlarging the equilibrium untilted unit cell in x-, y-, and both axes. For low values of area per molecule, i.e. high concentrations and surface pressure values, the untilted structures are the most energetically favorable and, hence, the more likely to appear, in coincidence with the experimental observations. At intermediate or large values of the area per molecule (low surface concentrations), different structures may appear depending on the type of deformation of the unit cell. In the case of enlarging along the y-axis, the minima structures correspond to carbon chains tilted along this axis, i.e. NNN tilted structures, with a  $b_\perp/a_\perp$  ratio pertaining to a herringbone (HB) configuration, ca. 1.4, features that coincide with those of the  $L_2'$  phase. In the case of elongation along the x-axis, minimum structures correspond to carbon chains tilted along this axis, i.e. NN tilted structures, with an  $b_\perp/a_\perp$  ratio pertaining to a herringbone (HB) configuration, ca. 1.3, are also predicted, features that coincide with those

of the  $L_2''$  phase. In general, when the distortion of the cell is only along one axis, the molecules tilt along this axis to preserve the intermolecular chain distances, and  $b_{\perp}/a_{\perp}$  ratio typical of the HB structures is obtained. However, in the last case (elongations along the x-axis), other minimum structures with inclinations along both axes are also found, which show transversal unit cell values similar to tilted phases with pseudo-herringbone (PHB)  $b_{\perp}/a_{\perp}$  ratio 1.7-1.8.

When the elongation of the unit cell is in both axes, structures with inclinations along both axes and HB  $b_{\perp}/a_{\perp}$  ratio are obtained.

Our calculations also show that transversal unit cell for the lowest energy configurations show similar  $b_{\perp}/a_{\perp}$  ratios in all the different areas per molecule selected in agreement with the experimental findings [17]. In addition, the tilt angle of the minimum structures, independently of the way that the untilted unit cell is deformed, changes rapidly from  $0^\circ$  to  $30^\circ$  when the area per molecule is augmented from 17.5 to 19  $\text{\AA}^2$ . This fact is in good qualitative agreement with the experimental observations, where the transition of untilted to tilted phases occurs at values of the area per molecule in the range of 20-23  $\text{\AA}^2$  [13]. The differences could again be due to our calculations are not taking into account temperature or solvation effects.

As summary, we can connect the calculation results to the structures observed in the phase diagram of the fatty acid monolayers (Figure 1). According to the results reported in Section 3, four different types of monolayer structures may be expected:

- i. Untilted structures at high concentrations with similar **a** and **b** values for all the fatty acids studied.
- ii. Structures which present unit cell distorted along either the x-axis or y-axis with tilt angles along the corresponding axis: NN-tilt (row 2 in Figure 6), and NNN-tilt (row 3 in Figure 6), respectively. In these two cases, the transversal unit cells obtained show a HB configuration ( $b_{\perp}/a_{\perp}$  ratios of ca. 1.3-1.5). These structures could be associated with the observed  $L_2''$  phase (with NN-tilt) in the case of tilt along the x-axis and the  $L_2'$  phase (with NNN-tilt) for the case of tilt along the y-axis. These kinds of

configurations yield energy minima for all the values of area per molecule explored, which might explain the wide range of concentrations in which both structures appear experimentally (see Figure 1).

- iii. Structures with tilt angles pointing to the y-axis but obtained from unit cell elongated only along the x-direction (row 4 in Figure 6). These monolayer structures could be associated with the  $L_{2h}$  phase, as they present a PHB configuration of the transversal unit cell ( $b_{\perp}/a_{\perp}$  ratios of ca. 1.7-1.8) and NN tilt. Moreover, such configurations are obtained only for low concentrations, in agreement with the fact that this phase is only observed at lower surface pressures [8]. In addition, according to our simulations at low concentration these structures are more likely to be observed than those associated with the  $L_2'$  phase (with HB parameters), because they are energetically more favorable. However, this difference is reduced when the concentration increase, becoming  $L_2'$  structures more stable for intermediate concentrations, in agreement with the experimental findings that show that the transition from  $L_2$  to the  $L_2'$  phase occurs when the concentration is increased [8, 29].
- iv. Structures with tilt pointing to mixed angles between x and y directions (shown in panel 4 of Figure 6) and unit cell distorted in both axes. However, we are not aware that these kinds of configurations have been observed yet. This can be due to the fact that when an intermediate distortion of the unit cell is produced, the different minima obtained (distorted in x-, y-, or both axes) are all connected by low energy barriers (lower than 0.1 eV, see figure 5 column 3). Consequently, the intermediate tilt structures could be considered as transition configurations that could evolve to tilted arrangements along x- or y- axis. When this evolution occur, the unit cell could instantly be distorted, recovering the configuration of x- or y-tilted phases, in which the energy barriers for a configuration transition are considerably higher (especially in the case of y-tilted structures), see Fig. 5 columns 1 and 2.

As a final remark, it has been mentioned along this manuscript that temperature and solvation effects could be the main responsible of the discrepancies between our calculated

and the observed parameters, as for example: the  $b_{\perp}/a_{\perp}$  ratio, surface concentrations or maximum inclinations angles of the tilted phases. In this context, we had carried out some test calculations to explore the nature of the dihydrogen interactions in fatty acid dimers. Preliminary results showed that the dihydrogen contacts established between hydrocarbon chains of the fatty acids are reinforced by the electron density of the polar heads, compared to the alike dihydrogen contacts established among hydrocarbon chain dimers (without polar head). This effect is stronger in the dihydrogen contacts which occur next to the polar head. This result is in agreement with the fact that larger unit cells are found for hydrocarbon chain structures. On the other hand, it is well known that when the aqueous medium is included in the calculations, the electron density of the polar head is shared with the water molecules [30]. This fact could cause that the dihydrogen contacts among hydrocarbon chain were weakened and consequently the **a** and specially the **b** axis (which present weaker interaction contacts and a higher intermolecular distance) of the unit cell were enlarger with respect to calculations which do not included the solvation effect. Indeed, larger **a** and especially **b** distances than our predicted values are experimentally observed. In addition, a thermal expansion of the dimensions of the unit cell is reasonably to occur when the temperature increase. Consequently, although more studies should confirm these hypotheses, it is reasonable to guest that temperature and solvation effect could increase the  $b_{\perp}/a_{\perp}$  ratio obtained by our calculations which in fact would provoke an increasing of the area per molecule and a decreasing of the maximum inclinations angles of the tilted phases.

## 5. Conclusions

We have performed a DFT study on the energetics and structures of the tilted phases of fatty acid Langmuir monolayers and their changes upon variation of the chain length, tilt

(both the angle and the azimuthal orientation), and area per molecule. The DFT method selected (in brief, a van der Waals vdW-DFT-cx functional with a large and flexible basis set) was recently proved to give good results in similar systems [16]. As far as we know, this is the first time that high level DFT methodology has been employed to simulate tilted phases of these systems.

Three different studies have been carried out. First, the effect of the chain length in the untilted phases of the monolayers has been analyzed, revealing that the unit cell dimensions for all the fatty acids studied (with chain lengths ranging from 10 to 20 carbon atoms) are quite similar. Second, we have explored the dependence of the energy of the unit cell on the inclination of the molecules (in the x and y axes), varying the surface concentration and keeping constant the transversal unit cell. This analysis has revealed that  $\Delta E$  variations are qualitatively similar for all the fatty acids studied (independent of chain length), showing an abrupt increase for inclinations larger than  $45^\circ$  ( $24 \text{ \AA}^2/\text{molecule}$ ) and  $36^\circ$  ( $21 \text{ \AA}^2/\text{molecule}$ ) for  $\phi_x$  (NN) and  $\phi_y$  (NNN), respectively, in qualitative agreement with the experimental findings. Third, we have studied the energetics and structures of the monolayer upon variation of the area per molecule. Such variation was imposed by enlarging the equilibrium untilted unit cell in x-, y-, and both axes. In this study, NN- NNN- (or even intermediate) tilted structures are obtained, which can be related with the different observed monolayer phases,  $L_{2h}$ ,  $L_{2'}$  and  $L_{2''}$ .

## Acknowledgments

O. T. acknowledges the Programa Operativo de Empleo Juvenil y la Iniciativa de Empleo Juvenil (YEI) of the Comunidad de Madrid for financial support under contract PEJ-2017-AI/AMB-6081. M.A. Rubio acknowledges the Ministerio de Ciencia, Innovación y



Universidades for financial support, under Grant FIS2017-86007-C3-3-P. Part of the calculations of this work has been carried out in the computational cluster of Dpto. of Física Fundamental of UNED. We thank to Dr. J. A. de la Torre and M. Pancorbo for the technical support in the use of the computational resources.

## REFERENCES

- [1] A. A. Sharipova, S. B. Aidarova, B. Z. Mutaliyeva, A. A. Babayev, M. Issakhov, A. B. Issayeva, G. M. Madybekova, D. O. Grigoriev and R. Miller, *Colloids and Interfaces*, 2017, **1**, 3.
- [2] N. Prabhakar, Z. Matharu and B. D. Malhotra, *Biosensors and Bioelectronics*, 2011, **26**, 4006-4011.
- [3] J. Liu, L. Zhang, Z. Xu and J. Masliyah, *Langmuir*, 2006, **22**, 1485-1492.
- [4] S. Schurch, J. Goerke and J. A. Clements, *Proc. Natl. Acad. Sci.*, 1976, **73**, 12, 4698-4702.
- [5] G. Ma and H. C. Allen, *Langmuir*, 2006, **22**, 5341-5349.
- [6] S. J. Marrink and H. J. C. Berendsen, *J. Phys. Chem.*, 1994, **98**, 4155-4168.
- [7] D. P. Tieleman, S. J. Marrink and H. J. C. Berendsen, *Biochimica et Biophysica Acta*, 1997, **1331**, 235-270.
- [8] V. M. Kaganer, H. Möhwald and P. Dutta, *Reviews of Modern Physics*, 1999, **71**, 3.
- [9] F. Bunel, J. Ignés-Mullol, F. Sagués and P. Oswald, *Soft Matter*, 2018, **14**, 4835-4845.
- [10] T. Verwijlen, L. Imperiali and J. Vermant, *Advances in Colloid and Interface Science*, 2014, **206**, 428-436.
- [11] D. Vollhardt, *Colloid & Interface Science*, 2014, **19**, 183-197.
- [12] V. M. Kaganer, I. R. Peterson, R. M. Kenn, M. C. Shih, M. Durbin and P. Dutta, *J. Chem. Phys.*, 1995, **102**, 23.
- [13] K. Kjaer, J. Als-Nielsen, C. A. Helm, P. Tippmann-Krayer and H. Möhwald, *J. Phys. Chem.*, 1989, **93**, 3200.
- [14] B. Lin, M. C. Shih, T. M. Bohanon, G. E. Ice and P. Dutta, *Phys. Rev. Letters*, 1990, **65**, 191.
- [15] R. M. Kenn, C. Böhm, A. M. Bibo, I. R. Peterson, H. Möhwald, J. Als-Nielsen and K. Kjaer, *J. Phys. Chem.*, 1991, **95**, 2092.
- [16] O. Toledano, O. Gálvez, *Phys. Chem. Chem. Phys.*, 2019, **21**, 21, 11203-11213,
- [17] I. Kuzemko, V. M. Kaganer and L. Leiserowitz, *Langmuir*, 1998, **14**, 3882-3888.
- [18] I. R. Peterson, V. Brzezinski, R. M. Kenn and R. Steitz, *Langmuir*, 1992, **8**, 2995-3002.

- [19] Y. B. Vysotsky, E. S. Kartashynska, E. A. Belyaeva, D. Vollhardt, V. B. Fainerman and R. Miller, *J. Phys. Chem. C.*, 2015, **119**, 5523–5533.
- [20] E. S. Fomina, Y. B. Vysotsky, E. A. Belyaeva, D. Vollhardt, V. B. Fainerman and R. Miller, *Journal of Physical Chemistry C*, 2014, **118**, 4122-4130.
- [21] Y. B. Vysotsky, E. S. Fomina, E. A. Belyaeva, D. Vollhardt, V. B. Fainerman and R. Miller, *Journal of Physical Chemistry C*, 2012, **116**, 26358-26376.
- [22] H. Rapaport, I. Kuzmenko, M. Berfeld, K. Kjaer, J. Als-Nielsen, R. Popovitz-Biro, I. Weissbuch, M. Lahav and L. Leiserowitz, *J. Phys. Chem. B*, 2000, **104**, 1399-1428.
- [23] K. Berland and P. Hyldgaard, *Phys. Rev. B: Condens. Matter Mater. Phys.*, 2014, **89**, 035412.
- [24] E. Schröder, V. R. Cooper, K. Berland, B. I. Lundqvist, P. Hyldgaard and T. Thonhauser, in *Non-Covalent Interactions, in Quantum Chemistry and Physics: Theory and Applications*, ed. A. O. de la Roza and G. A. de Labio, Elsevier Science, Amsterdam, 1st edn, 2017, ch. 8, pp. 241–274.
- [25] T. Thonhauser, V. R. Cooper, S. Li, A. Puzder, P. Hyldgaard and D. C. Langreth, *Phys. Rev. B: Condens. Matter Mater. Phys.*, 2007, **76**, 125112.
- [26] N. Troullier, Martin J.L., *Phys. Rev. B*, 1991, **41**, 1993-2006.
- [27] S. Tsuzuki, K. Honda, T. Uchimarui and M. Mikami, *J. Chem. Phys.*, 2006, **124**, 114304.
- [28] J. Pignat, J. Daillant, S. Cantin, F. Perrot and O. Konovalov, *Thin Solid Films*, 2007, **515**, 5691–5695.
- [29] J. Tajuelo, E. Guzmán, F. Ortega, R. G. Rubio and M. A. Rubio, *Langmuir*, 2017, **33**, 4280–4290.
- [30] L.F. Pacios, P.C. Gómez, and O. Gálvez, *Journal of Computational Chemistry*, 2006, **27** (14): 1650-1661.